Environmental Science & Technology

Article

pubs.acs.org/est

Linking Surface Urban Heat Islands with Groundwater Temperatures

Susanne A. Benz,*[,†] Peter Bayer,[‡] Frank M. Goettsche,[§] Folke S. Olesen,[§] and Philipp Blum[†]

[†]Karlsruhe Institute of Technology (KIT), Institute for Applied Geosciences (AGW), Kaiserstr. 12, 76131 Karlsruhe, Germany

[‡]ETH Zurich, Department of Earth Sciences, Sonneggstr. 5, 8092 Zurich, Switzerland

[§]Karlsruhe Institute of Technology (KIT), Institute of Meteorology and Climate Research—Atmospheric Trace Gases and Remote Sensing (IMK-ASF), Hermann-von-Helmholtz-Platz 1, 76344 Eggenstein-Leopoldshafen, Germany

Supporting Information

ABSTRACT: Urban temperatures are typically, but not necessarily, elevated compared to their rural surroundings. This phenomenon of urban heat islands (UHI) exists both above and below the ground. These zones are coupled through conductive heat transport. However, the precise process is not sufficiently understood. Using satellite-derived land surface temperature and interpolated groundwater temperature measurements, we compare the spatial properties of both kinds of heat islands in four German cities and find correlations of up to 80%. The best correlation is found in older, mature cities such as Cologne and Berlin. However, in 95% of the analyzed areas, groundwater temperatures are higher than land surface temperatures due to additional subsurface heat sources such as buildings and their basements. Local groundwater hot spots under city centers and under industrial areas are not revealed by satellite-derived land surface temperatures. Hence, we propose an estimation method that relates groundwater temperatures to mean annual land-surface temperatures, building density, and elevated basement temperatures. Using this method, we are able to accurately estimate regional groundwater temperatures with a mean absolute error of 0.9 K.

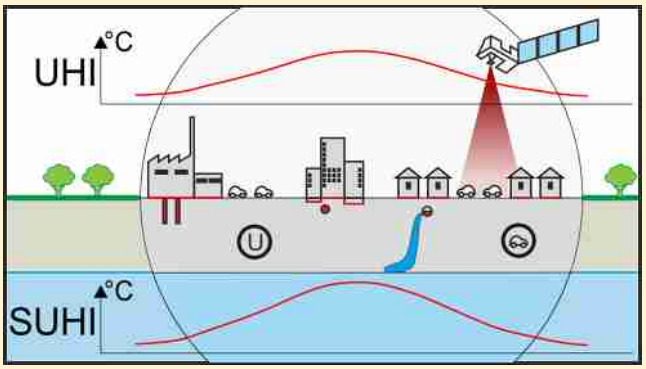

1. INTRODUCTION

In urban settlements, temperatures are typically, but not necessarily, elevated.[1] This so-called urban heat island (UHI) phenomenon exists in all layers of modern cities such as atmosphere, surface, and subsurface (SUHI). Various unfavorable issues are related to this phenomenon. The UHI on the surface is in part responsible for increased mortality rates during heat waves[2] and regional atmospheric pollution.[3] In contrast, the investigation of SUHI indicated some favorable qualities such as economic and ecological advantages for the use of shallow geothermal energy.[4] However, the increased groundwater temperatures also put stress on the underground ecosystems.[5] Until now, all layers are typically investigated individually, and information on the relationship between temperatures below and above ground is scarce.

The annual mean air temperature is closely related to the annual mean groundwater temperature due to conductive heat transport processes.[6−9] The timely correlation of subsurface temperatures and air temperatures has previously been shown by Cheon et al.[10] for four urban settlements in South Korea between 1960 and 2010. In addition, results from a study by Menberg et al.[11] demonstrated that the surface air temperature has a considerable impact on subsurface and groundwater temperatures (GWT). However, the coupling process between air and ground temperatures is not yet fully understood.[12,13]

Recently, satellite derived land surface temperatures (LST) has evolved as a new technique for above ground temperature measurements. Its relationships to air temperature and ground surface temperatures imply a correlation, but are not yet precisely determined.[14−17] However, satellite-derived LST enables easy access to the spatial and temporal conditions of UHIs, and it is therefore frequently applied in cities in India,[18] North America,[19] central Europe,[20] and worldwide.[21] In contrast, the spatial description of SUHIs relies on the interpolation of GWT measurements in existing groundwater monitoring wells and boreholes,[22−24] which is expensive and time-consuming. Especially in urban areas, groundwater wells are scarce and often too shallow (<15 m below ground) for characterizing SUHIs.

Thus, many studies try to estimate GWT from above ground measurements such as surface air temperature (2 m temperature) and/or LST.[25] Simulations of borehole temperatures from long-term measurements of surface air temperature or vice versa indicate promising results.[26−28] For example, Beltrami et al.[29] were able to reproduce 98% of the variance

Received: July 29, 2015
Revised: November 23, 2015
Accepted: November 23, 2015
Published: November 23, 2015

DOI: 10.1021/acs.est.5b03672
Environ. Sci. Technol. 2016, 50, 70−78

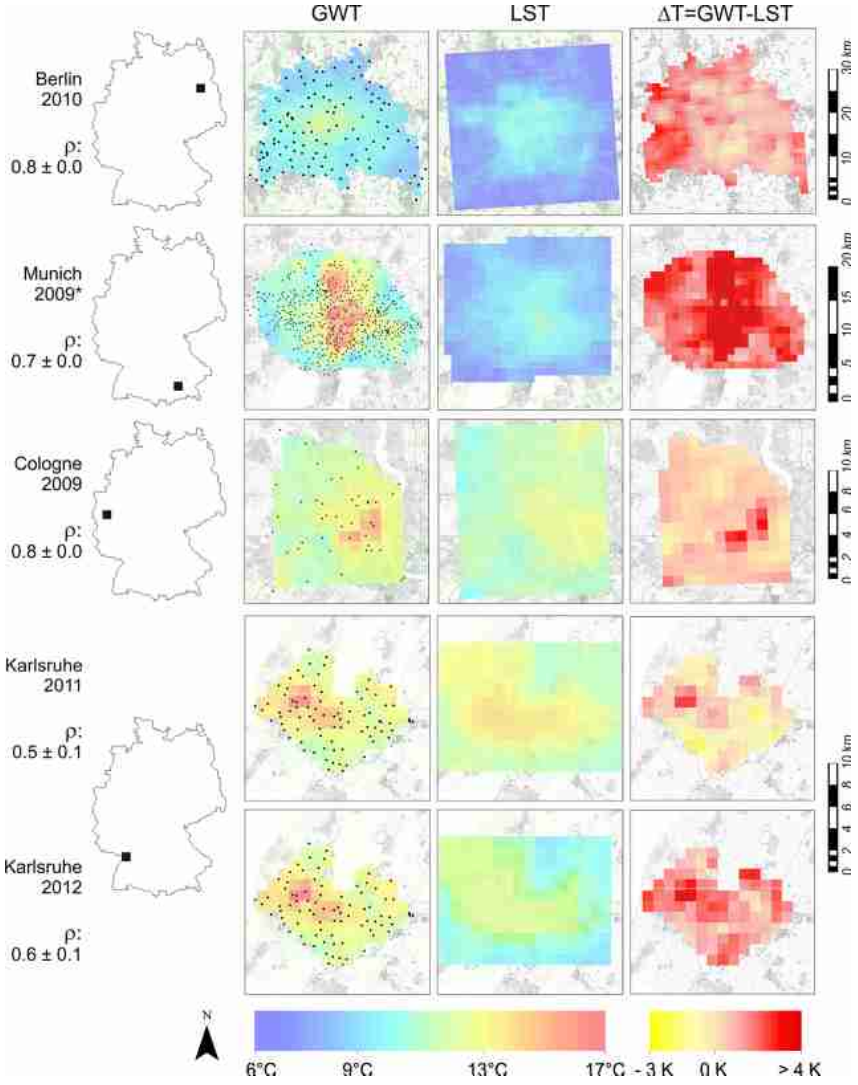

Figure 1. Geographical location, land surface temperature (LST), groundwater temperature (GWT), difference in temperatures (ΔT), and Spearman correlation (ρ) for all analyzed cities and years. Well locations are shown with GWTs. (Red) Positive ΔT represents a higher GWT, and (yellow) negative ΔT represents a higher LST.

in the borehole temperature using 70 years of surface air temperature in a rural area of Quebec. However, Huang et al.[30] showed that measured urban borehole temperatures were significantly elevated compared to those predicted from meteorological time series in Osaka, Japan. These deviations are caused by anthropogenic heat sources such as buildings and their basements, sewage systems, sewage leakage, subway tunnels, district heating networks, reinjection of thermal wastewater and geothermal energy systems.[24,31]

Zhan et al.[32] developed a one-dimensional (1-D) vertical heat transport model of Beijing's underground and reconstructed the subsurface thermal field at depths of 0.05, 0.40, and 3.20 m from satellite derived LST data. The results were validated with soil temperatures measured at seven ground-based sites for which the overall average mean absolute error for one year of daily temperatures was 1.5 K. However, due to the time delay between above- and below-ground temperatures and the lack of satellite data, modeling of deeper GWT was impossible. Furthermore, Zhan et al.[32] neglected below-ground anthropogenic heat fluxes into the subsurface, although recent studies showed that buildings and basements, as well as elevated ground surface temperatures, thermally dominate alterations of the urban underground.[33,34] In cities with a shallow groundwater table, heat flow from buildings can be more than double the heat flow from elevated ground surface temperatures.[33] Hence, for an improved estimation of urban GWT, the effects of buildings and urban infrastructure need to be considered. Furthermore, Zhu et al.[35] demonstrated that advection from horizontal groundwater flow is a crucial heat transport mechanism in the subsurface of Cologne. Thus, it must be considered when reconstructing the thermal environment of the urban underground.

The main objective of this study is to develop a method to estimate urban groundwater temperatures (GWT) from satellite-derived data. First, we compare urban heat islands (UHI) and subsurface urban heat islands (SUHI) in four German cities and analyze their dissimilarities in order to understand the interaction between the urban surface and subsurface. Spatial correlation and absolute differences between land surface temperatures (LST) and GWTs are carefully evaluated and the key drivers for the correlations are identified in an effort to analyze the interplay of UHI and SUHI. Second, we estimate annual mean urban GWT from annual mean satellite-derived LST and building densities of the studied cities.

DOI: 10.1021/acs.est.5b03672
Environ. Sci. Technol. 2016, 50, 70−78

Table 1. General Information on the Four Studied Cities and Years

	Berlin	Munich	Cologne	Karlsruhe	Karlsruhe
year studied	2010	2009	2009	2011	2012
year founded	1237	1158	38 B.C.	1715	1715
area (km^2)	891.7[a]	310.7[b]	405.2[c]	173.5[d]	173.5[d]
population	3 460 700[a]	1 364 200[b]	1 020 000[c]	303 000[d]	307 000[d]
population density (km^{-2})	3881	4391	2517	1746	1769
analyzed area (pixel)	928	437	147	89	88
groundwater flow velocity (m/d)[e]	0.03−1.4	10−15	ca. 1.0	0.5−3.5	0.5−3.5
groundwater depth (m)	1−10	0−22	3−22	2−10	2−10
measurement depth (m)	15	1−23	20	5−14	5−14
air temperature (°C)[f]	8.9	9.1	10.7	11.8	11.2

[a]Office for Statistics, Berlin-Brandenburg (Amt für Statistik Berlin-Brandenburg). [b]Office for Statistics, Munich (Statistisches Amt München). [c]Office for Urban Develpoment and Statistics, Cologne (Stadt Köln, Amt für Stadtentwicklung and Statistik). [d]Office for Urban Development, Karlsruhe (Stadt Karlsruhe, Amt für Stadtentwicklung). [e]Menberg et al.[31] [f]German Weather Service (Deutscher Wetterdienst, DWD).

Table 2. Summary of the Main Outcomes[a]

		Berlin (2010)	Munich (2009)	Cologne (2009)	Karlsruhe (2011)	Karlsruhe (2012)
annual mean temperature and standard deviation (°C)	Gwt	9.9 ± 0.8	11.9 ± 1.7	12.4 ± 1.0	13.0 ± 1.0	13.1 ± 1.0
	LST	8.7 ± 1.1	8.8 ± 0.8	11.7 ± 0.6	12.4 ± 0.8	11.1 ± 0.8
	eGWT	9.8 ± 1.6	10.2 ± 1.3	12.5 ± 1.0	13.6 ± 0.8	12.3 ± 0.9
	$eGWT_{Flow}$			12.6 ± 1.0	13.7 ± 0.7	12.5 ± 0.8
correlation and standard deviation	GWT/LST	0.77 ± 0.01	0.74 ± 0.03	0.83 ± 0.03	0.48 ± 0.08	0.62 ± 0.07
	GWT/eGWT	0.74 ± 0.02	0.74 ± 0.03	0.81 ± 0.04	0.49 ± 0.08	0.56 ± 0.08
	$GWT/eGWT_{Flow}$			0.87 ± 0.02	0.57 ± 0.09	0.66 ± 0.07
RMSE (K)	GWT/eGWT	1.1	2.1	0.7	1.0	1.2
	$GWT/eGWT_{Flow}$			0.6	1.0	1.2
MAE (K)	GWT/eGWT	0.9	1.8	0.6	0.8	1.0
	$GWT/eGWT_{Flow}$			0.5	0.8	0.9

[a]Shown are annual mean values of groundwater temperatures (GWT), land surface temperatures (LST), and estimated groundwater temperatures without (eGWT) and with flow ($eGWT_{FLOW}$), correlation and corresponding standard deviation (obtained via bootstrap method) and the accuracy of the estimated eGWT and $eGWT_{FLOW}$.

For two cities, this estimation method is then extended to include horizontal groundwater flow. These estimations allow for a first assessment of the SUHI and consequently the geothermal potential and groundwater ecological conditions, without the need for groundwater temperature measurements and data interpolation.

2. MATERIALS AND METHODS

Four German cities are chosen as study areas: Berlin, Munich, Cologne, and Karlsruhe (Figure 1, Table 1). From these, Karlsruhe stands out as being both the significantly smallest and youngest city. While Berlin, Munich and Cologne have more than 1 million inhabitants, Karlsruhe only has slightly more than 300.000. A single year of data for the three German megacities is analyzed; for Karlsruhe, two consecutive years (2011 and 2012) are analyzed, which also allows for the investigation of potential time-dependent changes. In the following, a brief overview of the hydrogeological properties and the GWT measurements of the studied cities is provided.

2.1. Hydrogeology and Groundwater Temperature. In general, the seasonal temperature fluctuations get damped and show a certain time lag in the unsaturated zone, which depends on the effective thermal diffusivity.[6] The penetration depth of this seasonal temperature fluctuation is also a function of the effective thermal diffusivity and typically ranges between 10 and 15 m[6]. In the present study, the focus is merely on annual mean temperatures that can be considered constant over certain depth. With increasing depth, however, the groundwater temperature is governed by the geothermal gradient at the site. Consequently, annual mean temperatures can be determined by either repeated measurements at shallow depths or a single measurement in a depth below the penetration depth of seasonal temperature fluctuation.

Berlin is located in the flat river Spree valley surrounded by two minor high points in the south and north. Both consist mainly of marly until and they are separated by the sandy glacial Spree valley. In this valley, the groundwater hydraulic head is between 1 and 10 m below the surface, while the groundwater table goes down to 40 m below surface under the two hills.[36] In 2010, GWT was manually measured in 123 wells by the Department for Urban Development and the Environment at depths of 15 m below ground.[37]

The subsurface of Munich consists mainly of gravel and cobble, and an unconfined aquifer.[31,38] The groundwater level reaches up to 1 m below the surface in the north and close to the Isar River. Only in the far south of the city is the groundwater level at 18 m below the surface. In October 2009, groundwater temperatures (GWT) were measured in 492 wells by the Environmental Department of Munich, but the measurements were taken only 1 m below the groundwater surface. Hence, these measurements are most probably influenced by seasonal temperature oscillations because they were elevated for this month compared to the annual mean values. To emphasize this bias, the data for Munich is marked with an asterisk (e.g., 2009*) in the present study and is not considered in the derivation of the estimation method.

DOI: 10.1021/acs.est.5b03672
Environ. Sci. Technol. 2016, 50, 70−78

In Cologne, the shallow subsurface also consists mainly of gravels and sands,[39] with the groundwater level at approximately 10 m below ground surface. GWTs were measured between September and October 2009 in 52 wells at 20 m below the surface using SEBA KLL-T logging equipment. The SUHI of Cologne was previously described comprehensively by Zhu et al.,[35] Menberg et al.,[31] and Benz et al.[33]

The shallow subsurface of Karlsruhe is also dominated by gravels and sands.[40] However, here the average groundwater level is only at 5 m below ground. GWT were measured 2−3 m below the groundwater surface in 82 wells by the Public Works Service of Karlsruhe. The wells are equipped with an Ackerman WPS05 data logger that records daily temperatures at 7 am. From these measurements, annual means for 2011 and 2012 were determined. The SUHI and the spatially variable subsurface anthropogenic heat fluxes of Karlsruhe have previously been described by Menberg et al.[37] and Benz et al.[33]

In the four studied cities, GWTs were interpolated with the same resolution as the available LST data (~1 km) using Kriging in GIS (ESRI ArcInfo, Version 10.1). Mean temperatures and their standard deviations and measurement years are compiled in Table 2.

2.2. Land Surface Temperature. Eight-day mean land surface temperatures (LST) were taken from the **Mod**erate **R**esolution **I**maging **S**pectroradiometer (MODIS) level-3 products, MOD11A2 and MYD11A2,[41,42] as obtained from NASA's TERRA and AQUA satellites, courtesy of the NASA Land Processes Distributed Active Archive Center (LP DAAC), USGS/Earth Resources Observation and Science (EROS) Center, Sioux Falls, South Dakota, https://lpdaac.usgs.gov.[43] They are composed of the daily 1 km product of both satellites. TERRA passes the study areas daily at approximately 10:30 am and pm, and AQUA at approximately 1:30 am and pm. LST is retrieved only for clear sky observations. Out of these, the annual arithmetic mean was determined for all cities and years. MODIS-derived LSTs have been previously validated by several studies[17,44−46] on the basis of ground-based and heritage satellite measurements. The annual mean MODIS LSTs are also given in Table 2.

The UHI of Berlin was discussed by Dugord et al.[47] They found a UHI magnitude [max LST − mean LST][48] of 8.7 K at 10:00 am and 3.2 K at 10:00 pm on August 14, 2000. In contrast, the annual mean UHI magnitude of Berlin determined for the year 2010 is only 2.8 K. This low value is expected due to the weak surface UHI in winter[49] that lowers the annual UHI magnitude compared to the summer.

2.3. Estimation Method. In rural areas, annual mean GWTs are often estimated using surface air temperatures, ground temperatures, or, recently, LSTs. However, in urban settlements, GWTs are also influenced by buildings[33] and other heat sources. Thus, it is impossible to estimate annual mean GWT using solely above-ground temperature. Hence, we combine annual mean LSTs and basement temperatures (BT) according to the building density (bd) to estimate annual mean groundwater temperatures (eGWT). Basements are typically not cooled (i.e., air conditioned), and thus, LST was taken as the lower limit of eGWT leading to the following equation:

$$\mathrm{eGWT} = \max\begin{cases} \mathrm{LST} \\ \mathrm{LST}(1 - \mathrm{bd}) + \mathrm{BT} \times \mathrm{bd} \end{cases} \quad (1)$$

Building densities were determined at the resolution of LST using building locations provided by OpenStreetMap[50] (Figure 4). In Germany, ground slab isolation was not implemented into construction regulation until the late 1990s,[51] and thus, additional thermal insulation of buildings is not considered here. Basement temperatures were estimated to be 17.5 ± 2.5 °C following guidelines by the German Institute for Standardization.[52] Additionally, building density and LST were assumed to be free of error.

To account for advective heat transport due to horizontal groundwater flow, the estimated groundwater temperature (eGWT) from satellite derived land surface temperature (LST) and building density is shifted according to the velocity and direction of the temperature signal in Cologne and Karlsruhe. At these locations, the flow can be considered constant over the entire study area. A detailed description of the calculation method can be found in the Supporting Information.

3. RESULTS

3.1. Comparison of Groundwater Temperature (GWT) and Land Surface Temperature (LST). Table 2 summarizes the main outcomes of this study, including mean values for GWTs and LSTs. Of the four analyzed cities, Berlin is the coldest (GWT: 10 °C; LST: 9 °C) and Karlsruhe, 2011, the warmest (GWT: 13 °C; LST: 12 °C). A map of GWTs, LSTs, and the difference ΔT of both temperatures and the Spearman correlation coefficient between GWT and LST are shown in Figure 1. The correlation coefficient for all cities and years ranges from 0.5 ± 0.1 for Karlsruhe, 2011, to 0.8 ± 0.0 for Cologne, 2012. All p-values are below 0.01, indicating statistical significance. In the four studied cities, GWTs indicate local hotspots which are not observed in the satellite-derived LST data. In Berlin, Cologne, and Karlsruhe, these hotspots are especially distinct and occur mainly under the city center where building densities are the highest. Moreover, in Cologne the hotspot can be directly linked to specific groundwater wells located next to the subway system and areas of local high sewage leakages.[33,53] These anthropogenic heat sources affect GWT but have no or only minor effects on above-ground temperatures. Similarly, the rise in GWT in the northwest of Karlsruhe is due to several existing reinjection wells of thermal wastewater.[37] This anthropogenically caused hotspot is particularly noticeable in 2011, when the LST was significantly higher than its long-term average (Table 2). The mean annual GWTs do not respond to such short-term changes in temperature, and therefore do not significantly deviate from their long-term mean. Still, the GWT close to the reinjection wells is about 3 K warmer than the LST over the entire area.

In Munich, the largest negative difference in temperature (ΔT) is due to the GWT measurements itself, which were taken in October only 1 m below the groundwater surface, resulting in significant seasonal bias. Hence, Munich is not considered much further in detail here. Still, it is an important case to demonstrate the large influence of shallow sampling depth and time.

For 95% of the analyzed pixels of the four cities, GWT was higher than LST (Figure 2). Disregarding Karlsruhe, 2011, where LSTs were considerably higher than the long-term average, this number increases to 97.4%. This confirms that the mean annual GWT is influenced by subsurface anthropogenic heat sources and therefore cannot solely be estimated from LST. However, in the four studied cities, long-term LSTs provide minimum temperatures for estimating annual mean urban GWTs (eq 1). On average, the measured GWTs are 1.5 ± 1.1 K warmer than the satellite-derived LSTs.

DOI: 10.1021/acs.est.5b03672
Environ. Sci. Technol. 2016, 50, 70−78

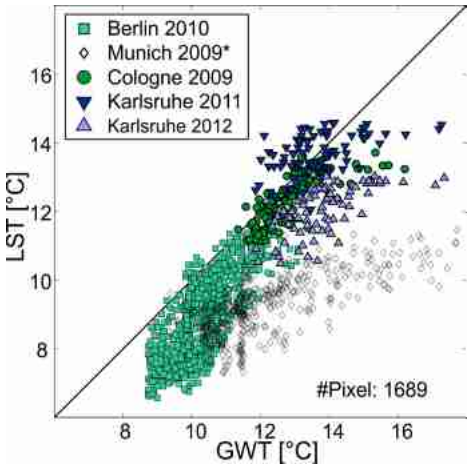

Figure 2. Comparison of groundwater temperature (GWT) and land surface temperature (LST) for all four analyzed cities. In 95% of the analyzed 1689 pixels, the GWT is higher than the LST.

3.2. Influences on the Correlation of UHI and SUHI.

Figures 3a–c show the influence of city- and year-specific parameters on the correlation coefficient ρ between groundwater temperature (GWT) and land surface temperature (LST; Figure 1). Only parameters that correlate to ρ with more than 85% and which have a p-value of <0.1 are shown. A list of all analyzed parameters is provided in Table S1 (Supporting Information). The largest correlation of 100% was found for the measurement depth in the groundwater (Table S1). This agrees with the fact that the influence of short-term anthropogenic heat sources such as road works or newly constructed buildings, and the seasonal oscillations of the LST decreases with depth.[6]

However, it is important to note that with increasing depth, groundwater temperatures are dominated by the natural heat flow (i.e., according to the geothermal gradient). Thus, the correlation between GWT and LST generally decreases with increasing measurement depth, depending on the vertical extension of the subsurface urban heat island (SUHI). The latter depends mainly on conductive heat transport and therefore on the age of the anthropogenic heat sources in the city. Accordingly, LST and GWT are better correlated for older and more mature urban settlements (Figure 3a). The size of the city also influences the observed relation between GWT and LST because pristine groundwater laterally enters the urban aquifer and influences the observed groundwater temperatures at the city border. With increasing size of the city, a smaller percentage of the area becomes affected and thus the influence on the overall correlation becomes minor (Figure 3b). However, due to the small sample size of four cities, major conclusions cannot be drawn and further research, including numerical simulations, should be performed to verify this interpretation.

3.3. Estimation of Groundwater Temperature.

The estimated groundwater temperature (eGWT) was determined from land surface temperature (LST) and building density according to eq 1 (Table 2). In Figure 4, the building density, the groundwater temperature (GWT), the eGWT, and the difference between estimated and measured GWT (ΔT) are shown for three analyzed cities. Because of its seasonally influenced GWT measurements, Munich is excluded from the detailed discussion. In short, the results for Munich show a mean annual eGWT of 10.2 °C, which is 1.7 K lower than the GWT measured in October 2009.

The correlation between GWT and eGWT shows no significant differences in the correlation between GWT and LST. Again, Karlsruhe—the smallest and youngest city—shows the lowest correlation, while Cologne—the oldest city with a study area roughly the size of Karlsruhe—has the largest correlation (ρ = 0.8). The estimated eGWT map displays the hotspots in the city center of the three investigated cities (Figure 4). However, as expected, the hotspot in the northwest of Karlsruhe, which is caused by local reinjections of thermal wastewater, cannot be determined using our proposed estimation method (eq 1). Similarly, the elevated GWT in the western part of Berlin cannot be identified either. Here, the building density is less than 2% and heat is most likely transported from the more densely populated city on top of the

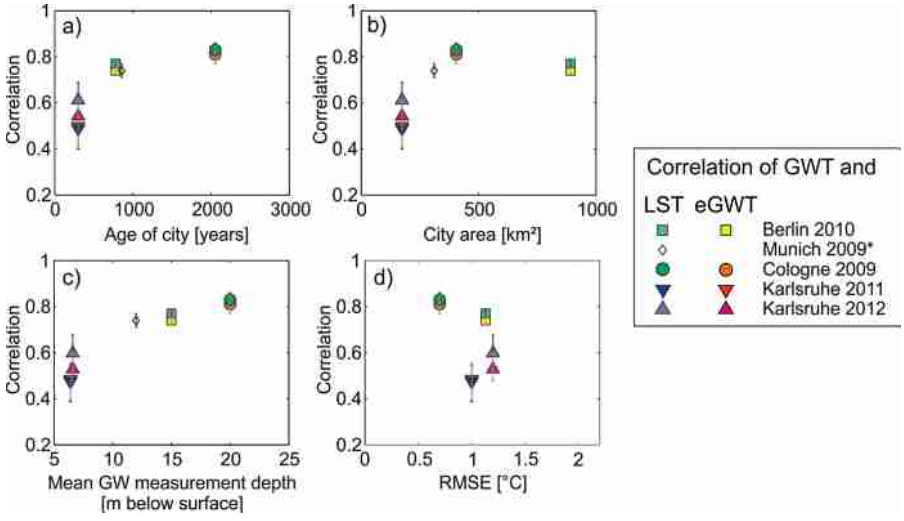

Figure 3. Spearman correlation coefficients (ρ) of groundwater temperature (GWT) and land surface temperature (LST), as well as of GWT and estimated groundwater temperature (eGWT), are plotted against several city-specific parameters. Mean groundwater measurement depth and the age of the city influence the correlation of GWT and LST the most, while RMSE and spatial correlation of GWT and LST seem independent of each other.

DOI: 10.1021/acs.est.5b03672
Environ. Sci. Technol. 2016, 50, 70–78

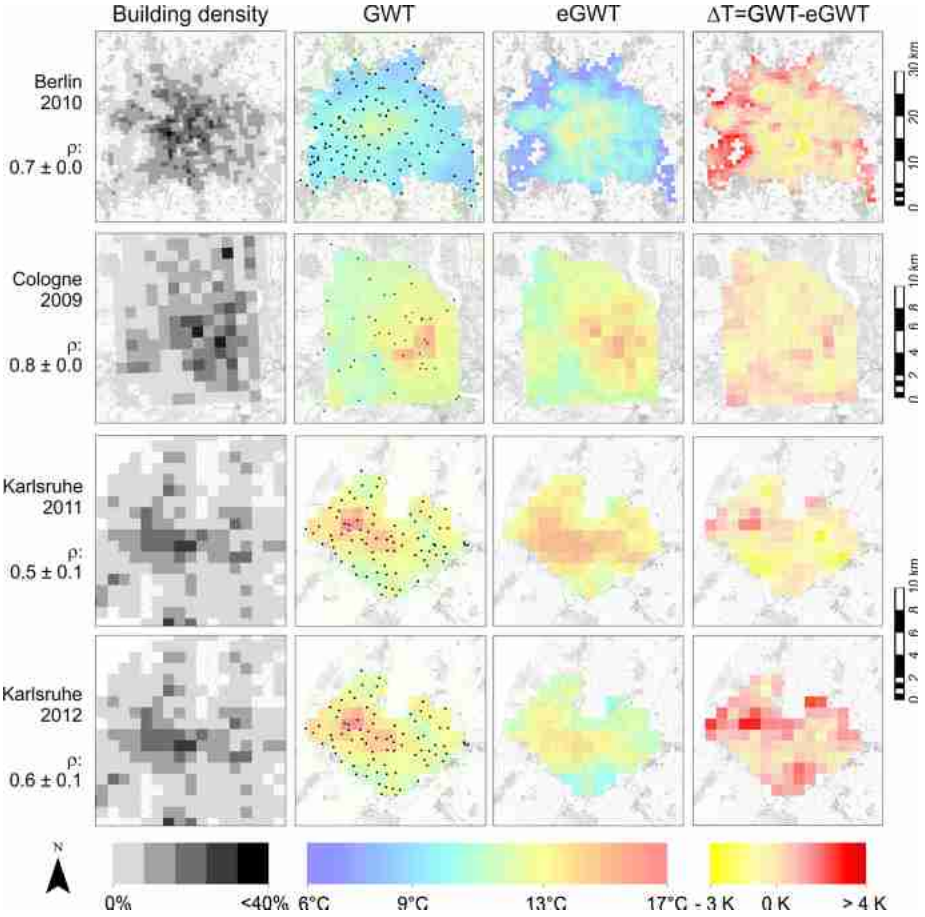

Figure 4. Building density, groundwater temperature (GWT), estimated groundwater temperature (eGWT), difference in temperatures (ΔT), and Spearman correlation (ρ) for all analyzed cities and years. Well locations are shown with GWTs. (Red) High ΔT represents a higher measured GWT, and (yellow) lower ΔT represents a higher estimated eGWT. Building densities were derived from building locations as given by OpenStreetMap.[50]

Tellow-Plateau into this western portion which is located in a valley.[54] It is also possible that other unidentified heat sources cause this local hotspot.

Overall, the deviation between measured and estimated GWT is minor and results in an average RMSE of 1.1 K (Figure 5). The error bars in Figure 5 represent the range of estimated

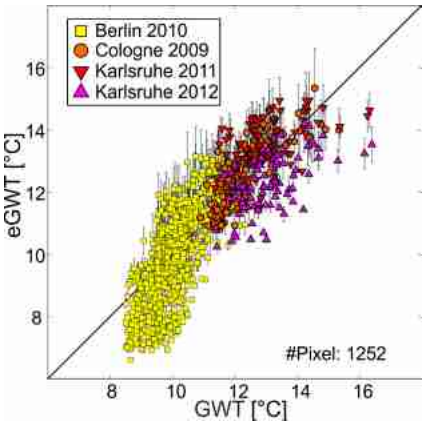

Figure 5. Comparison between measured groundwater temperatures (GWT) and estimated groundwater temperatures (eGWT). Error bars represent the assumed range due to uncertain basement temperatures. The overall mean absolute error is 0.9 K.

eGWT and stem from the assumed range of basement temperatures. Taking into account that the average range spans over 0.3 ± 0.2 K, the estimated eGWT range deviates on average by 0.6 ± 0.6 K from the measured temperatures.

It is important to note that a good RMSE does not necessarily mean that GWT and LST correlate spatially (Figure 3d). Berlin, for example, has a significantly higher correlation than Karlsruhe. However, when comparing the absolute values of eGWT, estimations for Karlsruhe agree slightly better with measured GWTs. The relatively low correlation of GWT and LST in Karlsruhe can be explained by the anthropogenic hotspot in the northwest, which is disproportionally weakening the correlation due to the small size of the city and the high velocity of the groundwater flow (Table 1).

Hence, the GWT-LST correlation for Karlsruhe increases by up to 0.1 if the groundwater flow is taken into account. Figure 6 shows maps of the estimated groundwater temperature with flow ($eGWT_{FLOW}$), as well as the temperature difference ΔT = GWT − $eGWT_{FLOW}$. For both analyzed cities the correlation is improved by 6 to 10% (Table 2). In contrast, the RMSE between GWT and $eGWT_{FLOW}$ is only slightly improved by less than 0.1 K compared to the estimation without groundwater flow (Table 2 and Figure S1).

The mean absolute error (MAE) in this study is 0.9 K and therefore 0.7 K lower than in the study by Zhang et al.,[55] who utilized satellite-derived LST to reconstruct the subsurface

DOI: 10.1021/acs.est.5b03672
Environ. Sci. Technol. 2016, 50, 70−78

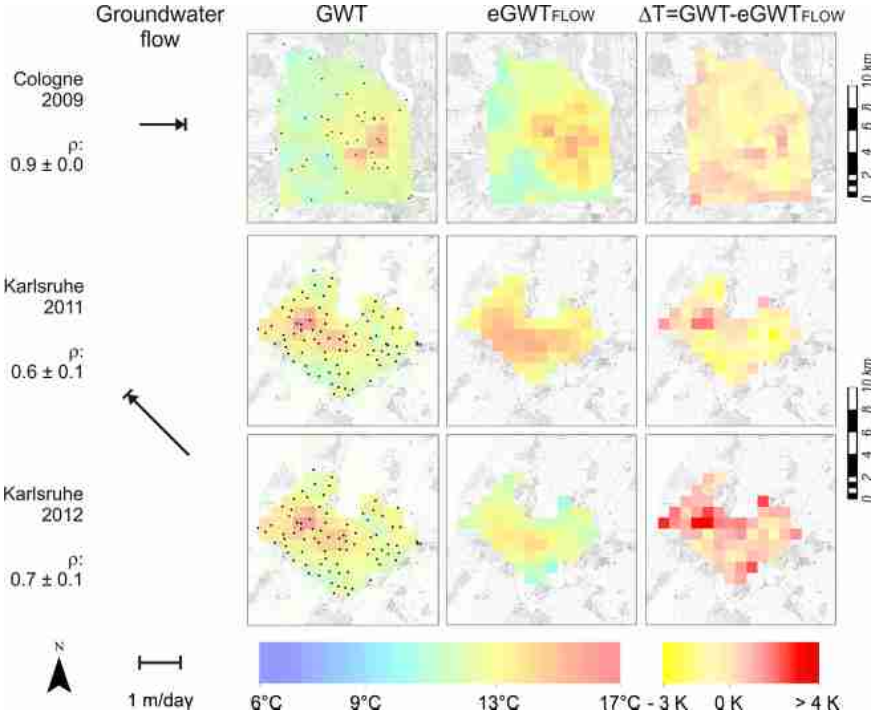

Figure 6. Groundwater flow, groundwater temperature (GWT), estimated groundwater temperature with groundwater flow ($eGWT_{FLOW}$), the difference in temperatures (ΔT), and Spearman correlation (ρ) for all analyzed cities.

thermal field of Beijing. However, they did not consider anthropogenic heat sources such as buildings and only estimated ground temperatures within a maximum depth of 3.20 m. We assume the remaining deviations between estimated and measured GWT stem from other anthropogenic sources rather than elevated surface temperatures and buildings. Benz et al.[33] found that 27% of the subsurface anthropogenic heat flow to the top of the groundwater surface in Cologne stems from sewage systems, sewage leakage, district heating networks, and the subway system, a considerable fraction that is not represented in our approach. For the year 2009, however, these heat sources alone could increase the groundwater temperature by approximately 0.1 K. Furthermore, this study considers only basements without insulation, which would result in an overestimation of GWT.

Our proposed estimation method combines land surface temperatures (LST) with basement temperatures to estimate groundwater temperatures (GWT) and improves the mean absolute error to a value of 0.9 K. In comparison, estimating GWT from LST alone results in an underestimation of 1.5 K. Hence, we conclude that mean annual urban GWT can be well approximated by combining satellite-derived LST data and building density (BD) data. The method allows investigations of subsurface urban heat islands (SUHI) and related issues such as geothermal potential[56] and groundwater quality where intensive GWT monitoring is not feasible. However, because the vertical extension of the SUHI appears to influence the correlation between above- and below-ground temperatures (Figure 3), we recommend applying the proposed estimation method to young mega-cities that are typically found in developing and BRIC countries (Brazil, Russia, India, and China). In principle, because LST and building density data are available from remote sensing, our method has the potential for large-scale and even global estimations of urban GWTs.

■ ASSOCIATED CONTENT

Supporting Information

The Supporting Information is available free of charge on the ACS Publications website at DOI: 10.1021/acs.est.5b03672.

Table S1, Figure S1, and a detailed description of the estimation method including horizontal groundwater flow. (PDF)

■ AUTHOR INFORMATION

Corresponding Author

*Phone: +49 721 608-47616. Fax: +49 721 606-279. E-mail: susanne.benz@kit.edu.

Author Contributions

The manuscript was written through contributions of all authors. All authors have given approval to the final version of the manuscript.

Notes

The authors declare no competing financial interest.

■ ACKNOWLEDGMENTS

The financial support for S.B. from the German Research Foundation (DFG) under grant number BL 1015/4-1 and the Swiss National Science Foundation (SNSF) under grant number 200021L 144288 is gratefully acknowledged. Furthermore, we thank Alexander Limberg and Thomas Scheider (Senate Department for Urban Development and the Environment, Berlin), Folker Dohr (Environmental Department, Munich), Stefan Jung (Karlsruhe Institute of Technology), and Susanne Reimer and Friedhelm Fischer (Public Work Service Karlsruhe) for their valuable support with data and additional information. Finally, we would like thank the two anonymous reviewers for their helpful comments.

DOI: 10.1021/acs.est.5b03672
Environ. Sci. Technol. 2016, 50, 70−78

ABBREVIATIONS

bd	building density
eGWT	estimated groundwater temperature
GWT	groundwater temperature
LST	land surface temperature
MAE	mean absolute error
RMSE	root-mean-square error
SUHI	subsurface urban heat island
UHI	urban heat island

REFERENCES

(1) Oke, T. R. City size and the urban heat island. *Atmos. Environ.* **1973**, *7* (8), 769−779.

(2) Gabriel, K. M.; Endlicher, W. R. Urban and rural mortality rates during heat waves in Berlin and Brandenburg, Germany. *Environ. Pollut.* **2011**, *159* (8−9), 2044−50.

(3) Sarrat, C.; Lemonsu, A.; Masson, V.; Guedalia, D. Impact of urban heat island on regional atmospheric pollution. *Atmos. Environ.* **2006**, *40* (10), 1743−1758.

(4) Allen, A.; Milenic, D.; Sikora, P. Shallow gravel aquifers and the urban 'heat island' effect: a source of low enthalpy geothermal energy. *Geothermics* **2003**, *32*, 569−578.

(5) Danielopol, D. L.; Griebler, C.; Gunatilaka, A.; Notenboom, J. Present state and future prospects for groundwater ecosystems. *Environ. Conserv.* **2003**, *30* (2), 104−130.

(6) Taylor, C. A.; Stefan, H. G. Shallow groundwater temperature response to climate change and urbanization. *J. Hydrol.* **2009**, *375* (3−4), 601−612.

(7) Kurylyk, B. L.; MacQuarrie, K. T. B.; McKenzie, J. M. Climate change impacts on groundwater and soil temperatures in cold and temperate regions: Implications, mathematical theory, and emerging simulation tools. *Earth-Sci. Rev.* **2014**, *138*, 313−334.

(8) Smerdon, J. E.; Pollack, H. N.; Cermak, V.; Enz, J. W.; Kresl, M.; Safanda, J.; Wehmiller, J. F. Daily, seasonal, and annual relationships between air and subsurface temperatures. *J. Geophys. Res.* **2006**, *111*, (D7).10.1029/2004JD005578

(9) Shi, B.; Tang, C. S.; Gao, L.; Liu, C.; Wang, B. J. Observation and analysis of the urban heat island effect on soil in Nanjing, China. *Environ. Earth Sci.* **2012**, *67* (1), 215−229.

(10) Cheon, J. Y.; Ham, B. S.; Lee, J. Y.; Park, Y.; Lee, K. K. Soil temperatures in four metropolitan cities of Korea from 1960 to 2010: implications for climate change and urban heat. *Environ. Earth Sci.* **2014**, *71* (12), 5215−5230.

(11) Menberg, K.; Blum, P.; Kurylyk, B. L.; Bayer, P. Observed groundwater temperature response to recent climate change. *Hydrol. Earth Syst. Sci.* **2014**, *18* (11), 4453−4466.

(12) Beltrami, H.; Kellman, L. An examination of short- and long-term air-ground temperature coupling. *Global and Planetary Change* **2003**, *38* (3−4), 291−303.

(13) Dědeček, P.; Šafanda, J.; Rajver, D. Detection and quantification of local anthropogenic and regional climatic transient signals in temperature logs from Czechia and Slovenia. *Clim. Change* **2012**, *113* (3−4), 787−801.

(14) Hachem, S.; Duguay, C. R.; Allard, M. Comparison of MODIS-derived land surface temperatures with ground surface and air temperature measurements in continuous permafrost terrain. *Cryosphere* **2012**, *6* (1), 51−69.

(15) Shamir, E.; Georgakakos, K. P. MODIS Land Surface Temperature as an index of surface air temperature for operational snowpack estimation. *Remote Sensing of Environment* **2014**, *152*, 83−98.

(16) Schwarz, N.; Schlink, U.; Franck, U.; Großmann, K. Relationship of land surface and air temperatures and its implications for quantifying urban heat island indicators—An application for the city of Leipzig (Germany). *Ecol. Indic.* **2012**, *18* (0), 693−704.

(17) Trigo, I. F.; Monteiro, I. T.; Olesen, F.; Kabsch, E. An assessment of remotely sensed land surface temperature. *J. Geophys. Res.* **2008**, *113*, (D17).10.1029/2008JD010035

(18) Chakraborty, S. D.; Kant, Y.; Mitra, D. Assessment of land surface temperature and heat fluxes over Delhi using remote sensing data. *J. Environ. Manage.* **2015**, *148*, 143−152.

(19) Hu, L. Q.; Brunsell, N. A. A new perspective to assess the urban heat island through remotely sensed atmospheric profiles. *Remote Sensing of Environment* **2015**, *158*, 393−406.

(20) Pongracz, R.; Bartholy, J.; Dezso, Z. Application of remotely sensed thermal information to urban climatology of Central European cities. *Phys. Chem. Earth* **2010**, *35* (1−2), 95−99.

(21) Peng, S.; Piao, S.; Ciais, P.; Friedlingstein, P.; Ottle, C.; Bréon, F.-M.; Nan, H.; Zhou, L.; Myneni, R. B. Surface Urban Heat Island Across 419 Global Big Cities. *Environ. Sci. Technol.* **2012**, *46* (2), 696−703.

(22) Taniguchi, M.; Shimada, J.; Fukuda, Y.; Yamano, M.; Onodera, S.; Kaneko, S.; Yoshikoshi, A. Anthropogenic effects on the subsurface thermal and groundwater environments in Osaka, Japan and Bangkok, Thailand. *Sci. Total Environ.* **2009**, *407* (9), 3153−64.

(23) Lubis, R. F.; Yamano, M.; Delinom, R.; Martosuparno, S.; Sakura, Y.; Goto, S.; Miyakoshi, A.; Taniguchi, M. Assessment of urban groundwater heat contaminant in Jakarta, Indonesia. *Environ. Earth Sci.* **2013**, *70* (5), 2033−2038.

(24) Ferguson, G.; Woodbury, A. D. Urban heat island in the subsurface. *Geophys. Res. Lett.* **2007**, *34* (23), L23713.

(25) Smerdon, J. E.; Pollack, H.; Cermak, V.; Enz, J. W.; Kresl, M.; Safanda, J.; Wehmiller, J. F. Air-ground temperature coupling and subsurface propagation of annual temperature signals. *J. Geophys. Res.* **2004**, *109* (21), D21107.

(26) Kooi, H. Spatial variability in subsurface warming over the last three decades; insight from repeated borehole temperature measurements in The Netherlands. *Earth Planet. Sci. Lett.* **2008**, *270* (1−2), 86−94.

(27) Huang, S.; Pollack, H. N.; Shen, P. Y. Temperature trends over the past five centuries reconstructed from borehole temperatures. *Nature* **2000**, *403* (6771), 756−8.

(28) Majorowicz, J.; Safanda, J. Measured versus simulated transients of temperature logs - a test of borehole climatology. *J. Geophys Eng.* **2005**, *2* (4), 291−298.

(29) Beltrami, H.; Ferguson, G.; Harris, R. N. Long-term tracking of climate change by underground temperatures. *Geophys. Res. Lett.* **2005**, *32* (19), 1−4.

(30) Huang, S.; Taniguchi, M.; Yamano, M.; Wang, C. H. Detecting urbanization effects on surface and subsurface thermal environment–a case study of Osaka. *Sci. Total Environ.* **2009**, *407* (9), 3142−52.

(31) Menberg, K.; Bayer, P.; Zosseder, K.; Rumohr, S.; Blum, P. Subsurface urban heat islands in German cities. *Sci. Total Environ.* **2013**, *442*, 123−33.

(32) Zhan, W.; Ju, W.; Hai, S.; Ferguson, G.; Quan, J.; Tang, C.; Guo, Z.; Kong, F. Satellite-derived subsurface urban heat island. *Environ. Sci. Technol.* **2014**, *48* (20), 12134−40.

(33) Benz, S. A.; Bayer, P.; Menberg, K.; Jung, S.; Blum, P. Spatial resolution of anthropogenic heat fluxes into urban aquifers. *Sci. Total Environ.* **2015**, *524*−*525*, 427−39.

(34) Epting, J.; Handel, F.; Huggenberger, P. Thermal management of an unconsolidated shallow urban groundwater body. *Hydrol. Earth Syst. Sci.* **2013**, *17* (5), 1851−1869.

(35) Zhu, K.; Bayer, P.; Grathwohl, P.; Blum, P. Groundwater temperature evolution in the subsurface urban heat island of Cologne, Germany. *Hydrological Processes* **2015**, *29* (6), 965−978.

(36) Hannappel, S.; Limberg, A. Ermittlung des Flurabstands des oberflächennahem Grundwassers in Berlin (Determination of the floor distance of shallow groundwater in Berlin). *Brandenburg. Geowiss. Beitr.* **2007**, *14*, 65−74.

(37) Menberg, K.; Blum, P.; Schaffitel, A.; Bayer, P. Long-Term Evolution of Anthropogenic Heat Fluxes into a Subsurface Urban Heat Island. *Environ. Sci. Technol.* **2013**, *47* (17), 9747−9755.

DOI: 10.1021/acs.est.5b03672
Environ. Sci. Technol. 2016, 50, 70−78

(38) Kerl, M.; Runge, N.; Tauchmann, H.; Goldscheider, N. Conceptual hydrogeological model of the City of Munich, Germany, as a basis for geothermal groundwater utilisation. *Grundwasser* **2012**, *17* (3), 127−135.
(39) Balke, K. D. *Geothermische und hydrogeologische Untersuchungen in der südlichen Niederrheinischen Bucht*. Bundesanstalt für Bodenforschung und den Geologischen Landesämtern der Bundesrepublik Deutschland: Hannover, 1973.
(40) Geyer, O. F.; Gwinner, M. P. *Geologie von Baden-Württemberg*. 5th ed.; Schweizerbart: Stuttgart, 2011.
(41) Wan, Z.; Dozier, J. A generalized split-window algorithm for retrieving land-surface temperature from space. *Geoscience and Remote Sensing, IEEE Transactions on* **1996**, *34* (4), 892−905.
(42) Wan, Z. MODIS Land-Surface Temperature. Algorithm theoretical basis document (LST ATBD): LST calculations. National Aeronautics and Space Administration: Washington, D.C., 1999.
(43) Land Processes Distributed Active Archive Center (LP DAAC), MODIS Level-3 1km Land Surface Temperature and Emissivity, Version 5. NASA EOSDIS Land Processes DAAC, USGS Earth Resources Observation and Science (EROS) Center: Sioux Falls, SD, https://lpdaac.usgs.gov.
(44) Ermida, S. L.; Trigo, I. F.; DaCamara, C. C.; Göttsche, F. M.; Olesen, F. S.; Hulley, G. Validation of remotely sensed surface temperature over an oak woodland landscape - The problem of viewing and illumination geometries. *Remote Sensing of Environment* **2014**, *148*, 16−27.
(45) Guillevic, P. C.; Biard, J. C.; Hulley, G. C.; Privette, J. L.; Hook, S. J.; Olioso, A.; Göttsche, F. M.; Radocinski, R.; Román, M. O.; Yu, Y.; Csiszar, I. Validation of Land Surface Temperature products derived from the Visible Infrared Imaging Radiometer Suite (VIIRS) using ground-based and heritage satellite measurements. *Remote Sensing of Environment* **2014**, *154*, 19−37.
(46) Wan, Z.; Zhang, Y.; Zhang, Q.; Li, Z.-l. Validation of the land-surface temperature products retrieved from Terra Moderate Resolution Imaging Spectroradiometer data. *Remote Sensing of Environment* **2002**, *83* (1−2), 163−180.
(47) Dugord, P. A.; Lauf, S.; Schuster, C.; Kleinschmit, B. Land use patterns, temperature distribution, and potential heat stress risk - The case study Berlin, Germany. *Computers, Environment and Urban Systems* **2014**, *48*, 86−98.
(48) Rajasekar, U.; Weng, Q. Urban heat island monitoring and analysis using a non-parametric model: A case study of Indianapolis. *ISPRS Journal of Photogrammetry and Remote Sensing* **2009**, *64* (1), 86−96.
(49) Schwarz, N.; Lautenbach, S.; Seppelt, R. Exploring indicators for quantifying surface urban heat islands of European cities with MODIS land surface temperatures. *Remote Sensing of Environment* **2011**, *115* (12), 3175−3186.
(50) OpenStreetMap; http://www.openstreetmap.org/copyright, http://www.openstreetmap.org, http://opendatacommons.org (accessed July 13, 2015).
(51) Deutsches Institut für Normung e.V. DIN 4108-2, 2011. Wärmeschutz und Energie- Einsparung in Gebäuden—Teil 2: Mindestanforderungen an den Wärmeschutz (Thermal protection and energy economy in buildings—Part 2: Minimum requirements to thermal insulation). Beuth Verlag GmbH: Berlin.
(52) Deutsches Institut für Normung e.V. DIN EN ISO 13370, 2008. Wärmetechnisches Verhalten von Gebäude—Wärmeübertragung über das Erdreich (Thermal performance of buildings—Heat transfer via the ground). Beuth Verlag GmbH: Berlin.
(53) Balke, K. D. *Die Grundwassertemperaturen in Ballungsgebieten*; Forschungsbericht−T81-028 (Institutional reasearch report T81−028); Geologisches Landratsamt Nordrhein−Westfahlen: Krefeld, 1981.
(54) Senate Department for Urban Development and the Environment, Berlin. Environmental Atlas, http://www.stadtentwicklung.berlin.de/umwelt/umweltatlas/edua_index.shtml, accessed July 4, 2015).
(55) Zhang, Y.; Choudhary, R.; Soga, K. Shallow geothermal energy application with GSHPs at city scale: study on the City of Westminster. *Géotechnique Letters* **2014**, *4* (2), 125−131.
(56) Zhu, K.; Blum, P.; Ferguson, G.; Balke, K. D.; Bayer, P. The geothermal potential of urban heat islands. *Environ. Res. Lett.* **2010**, *5* (4), 044002.

DOI: 10.1021/acs.est.5b03672
Environ. Sci. Technol. 2016, 50, 70−78